Harpur Hill, Buxton
Derbyshire, SK17 9JN
T: +44 (0)1298 218000
F: +44 (0)1298 218590
W: www.hsl.gov.uk

HEALTH & SAFETY LABORATORY

Large-Eddy Simulation of Gas Dispersion in a Room

HSL/2006/28

Project Leader: **M. J. Ivings**

Author(s): **S. E. Gant**

Science Group: **Fire & Explosion**

ACKNOWLEDGEMENTS

The author would like to thank Dr. Ian Jones, CFX Chief Technologist and Head of Technical Services (Ansys, Inc) for his useful comments and discussion of this report.

CONTENTS

EXECUTIVE SUMMARY

This report documents a preliminary study of gas dispersion in a room using Large-Eddy Simulation (LES), a relatively new computational modelling technique for application to industrial problems. The aim of this work has been to develop expertise in the new dispersion modelling technique and to examine the model's capabilities and limitations. The work forms part of a wider study aimed at developing dispersion modelling expertise for exposure assessment within HSE.

Over the last twenty years, the standard Computational Fluid Dynamics (CFD) approach for modelling gas dispersion in internal spaces has been to use "Reynolds Averaged Navier-Stokes" (RANS) models. These models solve for the *mean* or time-averaged flow parameters (mean air velocity, pressure, gas concentration etc.) rather than the real, instantaneous values. Whilst RANS models have the advantage of being relatively quick to calculate, they are also subject to modelling uncertainties and can only provide limited information on the statistical spread in values about the mean. The models can provide data on mean gas concentrations but cannot easily provide data on peak exposure levels.

Recent advances in computers have enabled more sophisticated turbulence models to be employed. Instead of calculating just the mean flow parameters, Large-Eddy Simulation CFD models determine the filtered instantaneous flow field and can therefore provide more information on peak gas concentrations. They still involve some modelling uncertainties since small-scale turbulent eddies are not resolved in the simulations. However, these uncertainties should be less significant than those of the RANS approach.

The case examined in this report is a room 4m by 4m by 2.7m high with a slot-shaped air inlet and ceiling extract. A similar configuration has previously been studied by HSL both experimentally and using RANS models [1, 2]. The room is initially filled with a uniform concentration of gas and gradually, over time, its concentration decreases as clean air enters the room and the gas/air mixture is extracted.

Three separate LES calculations and a RANS model calculation have been performed. Results are presented for the predicted gas concentrations near the exhaust over a period of 1000 seconds. The predicted gas concentration using LES follows the same overall trend as that of the RANS model, with marked fluctuations above and below the mean. These fluctuations provide information on the statistical spread in gas concentrations and give an indication of peak levels. The spatial resolution of the simulations is assessed according to a number of different criteria and details are provided of the computing time necessary to run the calculations.

The work shows that LES can provide a level of detail above and beyond that of standard RANS approaches in simulating gas dispersion in rooms. The cost of running LES calculations is still relatively high, with a single calculation taking a few weeks to run. Despite this, LES is starting to be used in safety cases and its use is likely to become more widespread as computers become more powerful and sufficiently cheap to be run in parallel. Likely future application areas for LES include the evaluation of scenarios for permitted uses of substances assessed under the REACH scheme.

It is recommended that expertise in LES be developed and maintained within HSE. In cases where detailed exposure assessments need to be made, LES should be considered as an alternative or as a complement to existing RANS models.

1 INTRODUCTION

Turbulence is a feature of practically all health and safety related fluid flows. To obtain reliable predictions of airborne contaminant transport it is essential that turbulence is modelled accurately. Computational Fluid Dynamics (CFD) is faced with considerable challenges in modelling turbulence. The difficulty arises from the range of spatial and temporal scales present in flows. In a typical room, eddies range in size from the order of millimetres up to tens of metres. The time scale for an eddy turnover may need a resolution of tenths of a second but it may also take a few hours for a full air change in the space. To resolve all of these scales directly using CFD requires computing resources way beyond today's capabilities. A recent review paper forecast that such direct approaches would not become feasible until 2070 [3].

Instead, the most commonly adopted computational modelling approach involves solving for the *mean* flow behaviour. By averaging the flow over a long time or over multiple snapshots, much of the eddy motion is smoothed out and so the resolution required in the simulation, both in space and time, is significantly reduced. This so-called "Reynolds Averaged Navier-Stokes" (RANS) approach has been widely used over the last 20 years for simulating gas dispersion and smoke movement in rooms (e.g. [4-6]). However, it is reliant upon empirical models to account for the effect of turbulence on the mean flow behaviour that can give rise to inaccuracies under certain flow conditions, such as laminar-turbulent transition. RANS models are also only able to return mean flow parameters, such as the mean gas concentration and cannot easily provide data on peak levels[1].

Advances in computing capabilities over the last decade have opened up the possibility of using more advanced and potentially more accurate turbulence models. A new approach called Large-Eddy Simulation (LES) is growing in popularity. LES has been demonstrated to perform well in a number of flows, notably in simulating gas dispersion in rooms and flow in street canyons [7-10]. Rather than averaging over time, LES involves averaging over a small, local region of space – a process known as 'filtering'. Effectively, the simulation uses a spatial resolution that is insufficient to capture all the fine, small eddies in the flow but the large, energy-containing flow structures are resolved fully. LES calculations are costly in terms of computing time since they need to resolve the unsteady motion of the large eddies and in many cases it is desirable to have a finer spatial resolution than that used with RANS models. The advantage of this, however, is that details of the turbulent fluctuations are returned and this can be used to provide information on peak exposure levels.

One of the uncertainties with LES is in assessing the level of spatial resolution obtained in a simulation, i.e. whether the solution is resolving all the large eddies or just the very large eddies. Section 2 of this report provides details of a number of measures that can be used to assess the spatial and temporal resolution of LES. These measures can be used to provide a quality check on the simulation.

In Section 3, LES is applied to one particular scenario relevant to exposure assessment: gas dispersion in a room. The work is not intended to be a thorough and detailed examination of LES performance but a brief look at its use in a relatively simple test case, to gain some appreciation of its benefits and costs.

[1] *Although RANS models contain data on mean-square fluctuations, there is no direct way in which peak values can be extracted without making further restrictive modelling assumptions.*

2 LARGE-EDDY SIMULATION: RESOLUTION ISSUES

The objective in running a large-eddy simulation is to resolve the large energy-containing flow structures and approximate or model the smaller, more uniform, eddies. In practice, when faced with a new flow scenario it is difficult to know *a priori* how coarse or fine to make the mesh. Using RANS models this problem does not usually arise, one simply runs a number of calculations with progressively finer grids until no differences are observed in the results. The same approach cannot be adopted in LES owing to the very significant computing costs involved. Instead, it is common practice to use just one or two different grids and put the effort into making these as fine as possible, given the available computing resources.

There is a clear need to be able to assess the quality of the grid used in large-eddy simulations, especially with regard to assessing LES used to support safety cases. Some practical guidance on the level of spatial and temporal resolution can be obtained from the following four parameters:

1. Ratio of turbulent length scales to grid cell dimensions
2. Dimensionless wall distances
3. Courant number (see page 4)
4. Ratio of the modelled to the total turbulent kinetic energy.

The first three of these parameters can be assessed (approximately) using results from a previous RANS simulation. They therefore provide guidance on the grid resolution without having first to perform the LES. The fourth measure can only be assessed once LES results have been obtained.

These four measures are described fully below. Technical details have been included to help inform future modelling efforts. For an introduction to the terminology used (subgrid stresses, dynamic models etc.), see for example Pope [11].

2.1 RATIO OF TURBULENCE LENGTH SCALES TO GRID CELL DIMENSIONS

The LES subgrid stress can be divided into two parts: an *isotropic* component which controls the rate of energy dissipation but does not affect the mean flow equations directly, and an *anisotropic* component which influences the mean shear stress and mean velocity profiles. There is a size-distribution of these stresses with smaller scale turbulence structures exhibiting more isotropic behaviour. According to Baggett *et al*. [12], the dynamic Smagorinsky model provides accurate predictions of the isotropic subgrid stress component (i.e. energy dissipation), but does not capture the correct anisotropic behaviour. Their study of channel flows using different grids showed that the subgrid stress predicted by the dynamic model was three to four times smaller than that obtained by filtering a DNS result (where the explicit filter applied to the DNS was proportional in each case to the cell size used in the LES). They attributed this poor performance to the inaccuracy of the model at capturing the correct anisotropic stresses.

To obtain accurate LES results they suggested that the grid should be sufficiently fine so that only the smaller, isotropic eddies are modelled. To achieve such conditions, they recommended that the modelled subgrid-scale (SGS) stress should account for only a negligible fraction of the total stress. Using this criterion, any errors due to the model should be insignificant.

To find out how this can be achieved in practice, they examined two flows: a non-equilibrium boundary layer with strong adverse pressure gradient and a circular jet. They showed that the SGS stress became essentially isotropic as the filter width, Δx , approached a certain fraction of the turbulence dissipation length scale:

$$\Delta x < \frac{L_\varepsilon}{10}$$

where $L_\varepsilon = \frac{q^3}{\varepsilon}$ and $q^2 = \overline{u_i u_i}$. The filter width in the above expression can be approximated as twice the cube-root of the cell volume $\left(\Delta x = 2(Vol)^{1/3}\right)$ and the trace of the Reynolds stress, $\overline{u_i u_i}$, can be written in terms of the turbulent kinetic energy, $k = \frac{1}{2}\overline{u_i u_i}$. Rearranging the above formula then gives:

$$2(Vol)^{1/3} < \frac{(2k)^{3/2}/\varepsilon}{10}$$

or, approximately:

$$(Vol)^{1/3} < \frac{k^{3/2}/\varepsilon}{10}$$

The above equation provides guidance on the appropriate grid size for large-eddy simulations. Values of k and ε can be found from a prior RANS calculation, using for instance a $k-\varepsilon$ model. This approach was used by Addad *et al*. [13] to examine LES grid resolution in a study of a negatively buoyant wall jet.

2.2 NEAR-WALL GRID RESOLUTION

The distance from the wall surface to the nearest node inside the flow domain, y, is commonly made dimensionless as follows:

$$y^+ = \frac{yU_\tau}{\nu}$$

where y^+ is the dimensionless wall distance, ν is the kinematic viscosity and U_τ is the friction velocity, defined as:

$$U_\tau = \sqrt{\frac{\tau_{wall}}{\rho}}$$

In the above expression, τ_{wall} is the resultant wall shear stress and ρ the density.

To fully resolve the boundary-layer with LES, the dimensionless cell spacing should be (Δx^+, Δy^+, Δz^+) < (10, 1, 50) in the spanwise, wall-normal and streamwise directions, respectively. In some cases, it may not be necessary to fully-resolve the boundary layer to obtain good overall flow predictions with LES. For example, when turbulence structures are predominantly generated by large geometrical features, buoyancy, free shear layers or flow curvature (e.g. [13]).

2.3 COURANT NUMBER

The Courant number, C, for one-dimensional flow is the ratio of the time step, Δt, to the characteristic convection time, $\Delta x/U$:

$$C = \frac{\Delta t}{\Delta x / U}$$

where U is the velocity in the x-direction and Δx is the cell width. For accuracy and numerical stability, the Courant number should ideally be less than unity everywhere. In complex three-dimensional flows with unstructured grids this condition can be approximated by:

$$C = \frac{|\mathbf{U}|}{(Vol)^{1/3}} \Delta t < 1$$

where $|\mathbf{U}|$ is the magnitude of the velocity vector.

If long time steps are used, such that the Courant number exceeds a value of one, undesirable numerical damping may be introduced into the solution. However, accurate results may still be obtained if the Courant number exceeds one, provided the flow is not changing significantly in the high C regions. Similarly, Courant numbers greater than one may occur in regions of the flow where the grid cells are very small, but this may not have a detrimental effect on the results.

2.4 MODELLED SUBGRID-SCALE TURBULENT KINETIC ENERGY

It was noted above that Baggett *et al.* [12] recommended the modelled SGS stress to account for a negligible fraction of the total stress. In a review of LES modelling for HSE, WS Atkins proposed a less stringent criteria [14]. They suggested that the ratio of the resolved turbulent kinetic energy, k_r, to the total turbulent kinetic energy, k, should be above 70% for 'medium' resolution LES and above 80% for 'well-resolved'. This is in agreement with Pope's comments that approximately 80% of the total turbulence energy should be resolved [11].

The total turbulent kinetic energy is represented by the sum of the resolved turbulent kinetic energy, k_r, and the modelled SGS kinetic energy, k_s:

$$k = k_r + k_s$$

In other words, the WS Atkins and Pope criterion for well-resolved LES is for:

$$\frac{k_r}{k_r + k_s} > 0.8$$

Details of how to calculate k_r and k_s are presented below.

2.4.1 Resolved Turbulent Kinetic Energy, k_r

In statistically-stationary flows, the instantaneous or total velocity, $\widetilde{U}$, can be decomposed into two parts: a mean component, U, and a fluctuation, u (as shown in Figure 1). The mean velocity, U, is calculated from a long time-average of the instantaneous value, $U = \overline{\widetilde{U}}$.

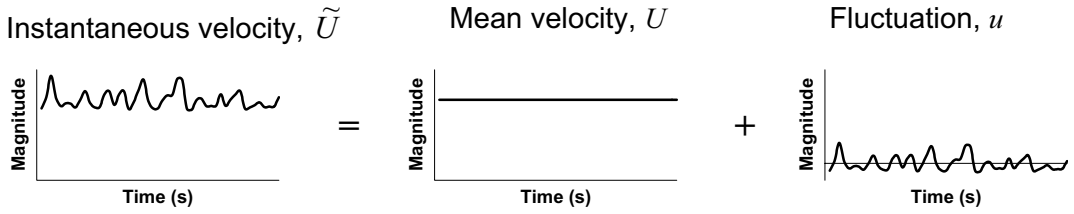

Figure 1 Decomposition of the instantaneous velocity field, $\widetilde{U}$, into the mean, U and fluctuation, u.

The square of the fluctuating velocity component in the three coordinate directions (uu, vv and ww) are averaged over time to find the resolved Reynolds stresses $\overline{u^2}$, $\overline{v^2}$ and $\overline{w^2}$. These are used to calculate the resolved turbulent kinetic energy, as follows:

$$k_r = \frac{1}{2}\left(\overline{u^2} + \overline{v^2} + \overline{w^2}\right)$$

There are a number of different approaches that can be used to find the *modelled* subgrid turbulent kinetic energy, k_s. Three alternatives are presented below: the first, based on simple velocity and length scale assumptions, the second from Pope [11] and the third from Mason & Callen [15].

2.4.2 Calculating the Modelled Turbulent Kinetic Energy, k_s, from Assumed Velocity and Length Scales (the *UL* Approach)

The Smagorinsky model calculates the subgrid-scale viscosity, ν_t, from:

$$\nu_t = \left(c_s \Delta\right)^2 \left|S\right|$$

where c_s is a constant, Δ is the filter width and S the strain-rate invariant. This can also be written as:

$$\nu_t = UL$$

where U and L are characteristic velocity and length scales of the unresolved subgrid-scale motion. These can be approximated as:

$$U = \sqrt{\frac{2}{3}k_s} \qquad\qquad L = \sqrt[3]{Vol}$$

where k_s is the modelled SGS turbulent kinetic energy and Vol is the volume of the finite-volume cell. The expression for U is derived from isotropic turbulence $\left(\overline{u_i u_i} = \frac{2}{3}k\right)$. Rearranging the above equations, the modelled subgrid turbulent kinetic energy can be calculated from:

$$k_s = \frac{3}{2}\left(\frac{\nu_t}{\sqrt[3]{Vol}}\right)^2$$

From now on, this approach will be referred to as the 'UL' approach.

2.4.3 Calculating the Modelled Turbulent Kinetic Energy, k_s: Pope's Approach

Pope [11] presents the following estimate for the ratio of the subgrid turbulent kinetic energy, k_s, to the total turbulent kinetic energy, k:

$$\frac{k_s}{k} = \frac{3}{2}C\left(\frac{\Delta}{\pi L}\right)^{2/3}$$

where C is the Kolmogorov constant, equal to 1.5, and L is the turbulence length scale, which can be approximated by $L = k^{3/2}/\varepsilon$. This expression is derived by considering a sharp spectral cut-off in the inertial subrange of high-Reynolds-number turbulence. The above formula can be rearranged to give:

$$k_s = \frac{3}{2}C\left(\frac{\Delta\varepsilon}{\pi}\right)^{2/3}$$

and the dissipation rate, ε, can be approximated by:

$$\varepsilon = \nu_t S^2$$

Assuming the filter width to be twice the cube-root of the cell volume $\left(\Delta = 2(Vol)^{1/3}\right)$, the modelled SGS turbulent kinetic energy can then be calculated from:

$$k_s = 3.6\left(\frac{\nu_t S^2 (Vol)^{1/3}}{\pi}\right)^{2/3}$$

2.4.4 Calculating the Modelled Turbulent Kinetic Energy, k_s: Mason & Callen's Approach

In their paper which examined the sensitivity of LES results to the magnitude of the Smagorinsky coefficient [15], Mason & Callen presented the following formula for the modelled subgrid-scale turbulence energy:

$$k_s = \frac{l^2 S^2}{C_E}$$

where S is the strain-rate, C_E is a constant stress-energy ratio which is assumed to have a value of 0.3 and l is the Smagorinsky length scale, given by:

$$l = c_s \Delta$$

In the present calculations, the Smagorinsky coefficient, c_s has been assigned a value of 0.1. Assuming, as before, that the filter-width is given by $\left(\Delta = 2(Vol)^{1/3}\right)$, the expression for the subgrid turbulence energy can be rearranged to give:

$$k_s = \frac{\left[0.2(Vol)^{1/3}\right]^2 S^2}{0.3}$$

Mason & Callen developed the above expression by assuming that subgrid-scale stresses were isotropic, along similar lines to the mixing-length RANS model. They noted that "[it] is only intended to give an appraisal of the general magnitude of the subgrid energy".

2.4.5 Modelled Turbulent Kinetic Energy, k_s: Summary

If one assumes that the subgrid-scale viscosity, ν_t, is obtained from the Smagorinsky model with coefficient, c_s = 0.1, the three methods presented above for calculating k_s can all be written as functions of the filter width $\left(\Delta = 2(Vol)^{1/3}\right)$ and strain-rate, S, as follows:

UL: $k_s = 0.0006\Delta^2 S^2$

Pope: $k_s = 0.049\Delta^2 S^2$

Mason & Callen: $k_s = 0.033\Delta^2 S^2$

All three methods agree that k_s should be a quadratic function of both Δ and S. Interestingly, the Pope and Mason & Callen formulae agree on the rough order-of-magnitude of k_s, whilst the UL method produces a value of k_s approximately 70 times smaller. It should be noted, however, that all three methods are only very approximate[2].

[2] *One source of discrepancy is that in some texts, the filter width Δ is taken as the cube-root of the cell volume, whereas in others it is assumed to be twice the cube-root of the cell volume.*

A recent example application of the above approach to determine the proportion of resolved turbulent kinetic energy is given in Kempf *et al*. [16]. They used a dynamic Smagorinsky model to determine c_s and found the resolved kinetic energy from:

$$k_s = \left(\frac{c_s}{0.1} \right)^2 \Delta^2 S^2$$

For the non-premixed combustion case studied, they found that results were poor when the resolved part, k_r, of the total turbulent kinetic energy, $k_r + k_s$, was less than 70%.

Comparisons of the proportion of resolved kinetic energy are presented in Section 3 for the gas dispersion test case where k_s is calculated using the UL and Pope methods.

3 GAS DISPERSION SIMULATION

3.1 FLOW GEOMETRY AND BOUNDARY CONDITIONS

The geometry of the room considered in this study is shown in Figure 2. Air enters the square green duct on the left-hand-side of the figure and flows into the diffuser-shaped plenum. From there, air exits through a narrow slot along the full width of the plenum at high level and flows into the room (shown in blue). Air is extracted from the ceiling of the room via a 20cm square orifice which leads into an exhaust duct (in red). A flat velocity profile is imposed at the face of the square inlet duct leading to the plenum which has an open area of 0.25 m^2. This flow rate is equivalent to a ventilation rate in the room of 2.1 air changes per hour (ach). Previous studies have examined the same room with ventilation rates of 0.5, 1 and 3 ach [1, 2]. The purpose of the inlet duct and plenum in the simulations is to obtain more representative inflow conditions than would be obtained by imposing boundary conditions directly on the room air inlet. As will be shown later, turbulent structures appear to be generated in the main room primarily by the strong shear layer in the wall jet. The flow behaviour in the inlet plenum may not, therefore, affect significantly the flow in the room.

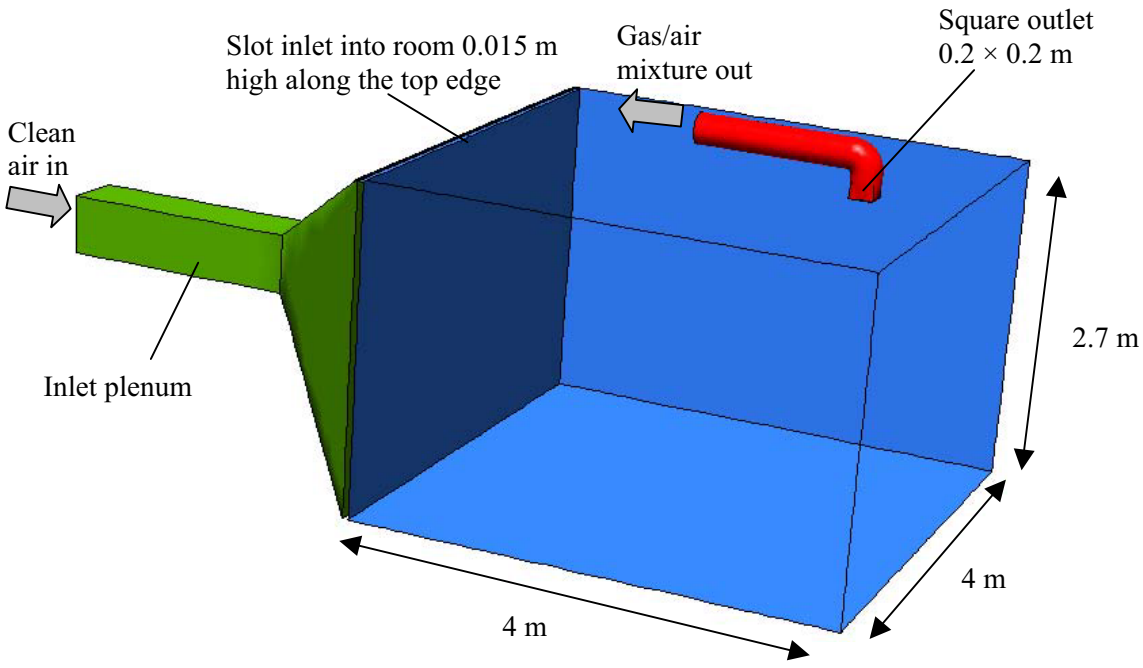

Figure 2 Room geometry

All of the walls in the room are adiabatic except the floor, which is maintained at a constant temperature of 16.5 ºC. Air enters the room at a temperature of 18.4 ºC. The difference between the supply air and floor temperatures forms a stable stratification in the room. The Boussinesq approximation is used to account for buoyancy in the CFD model. Air properties (density, viscosity, conductivity) are standard temperature and pressure (STP) values.

3.2 COMPUTATIONAL GRID AND DIFFERENCING SCHEMES

The grid used in this study is the same as that used previously in [2] for RANS model calculations. Plots of the side and end views are shown in Figure 3 below. A total of 193,316 nodes were used: 157,502 for the main room, 33,208 for the inlet plenum and 2606 for the exhaust duct.

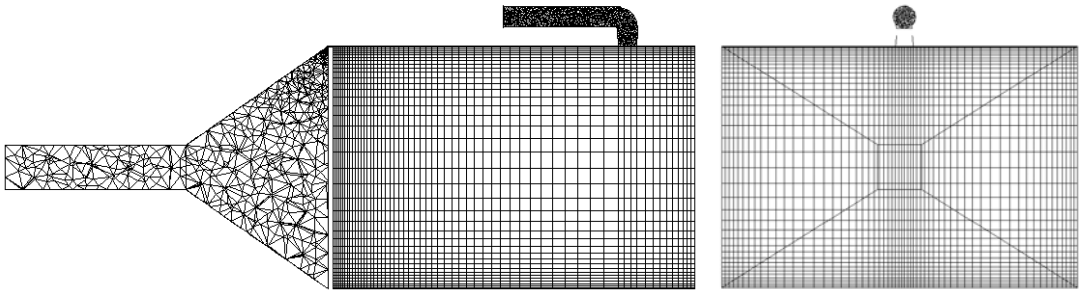

Figure 3 Side and end views of the computational grid in cross-section.

With LES, it is usually recommended that central differencing is used to discretize the convective terms in the transport equations, in order to conserve kinetic energy [17, 18]. Upwind schemes are known to be overly dissipative and can damp out small-scale eddy motion.

Tests using the above grid found that central differencing caused dispersive errors in the solution. This was manifested as unbounded predicted gas concentrations with peaks in excess of the initial gas concentration (despite there being no source of gas in the room). Temperatures also exhibited alternate high-low-high values in neighbouring cells. These errors suggest that the computational grid was probably too coarse.

To avoid this unphysical behaviour, a blend of central and upwind differencing was used in the gas concentration and energy equations, with 90% central and 10% upwind. Pure second-order central differencing was still used in the momentum equations. Second-order backwards Euler differencing in time was used for all variables except the gas concentration, which used first-order backwards Euler.

3.3 INITIAL CONDITIONS

It is important in running LES calculations to have the flow field initialised correctly. The approach taken here has been to use a pre-calculation, i.e. to run the LES for some time in order to obtain a representative flow field and only once fully-developed conditions have been achieved, then to initialise the contaminant gas field. Two pre-calculations were run: one starting from a previous RANS solution and another starting from the same RANS solution superimposed with random velocity fluctuations of magnitude 0.01m/s (10% of the room inlet velocity). The purpose of these random fluctuations was to kick-start the production of turbulent eddies. Figure 4 shows the flow development over a period of a minute using these two approaches.

Based on the results shown in Figure 4, it was decided to run the pre-calculation with superimposed fluctuations for a longer period of time and to use the resulting flow field as initial conditions for the gas dispersion calculations. The calculation was run on for a further 4

minutes and 50 seconds which was equivalent to 9 flow-through times, based on the mean velocity along the top of the room and the direct distance from inlet to outlet. Figure 5 shows the velocity monitored at 8 locations in the room over this period.

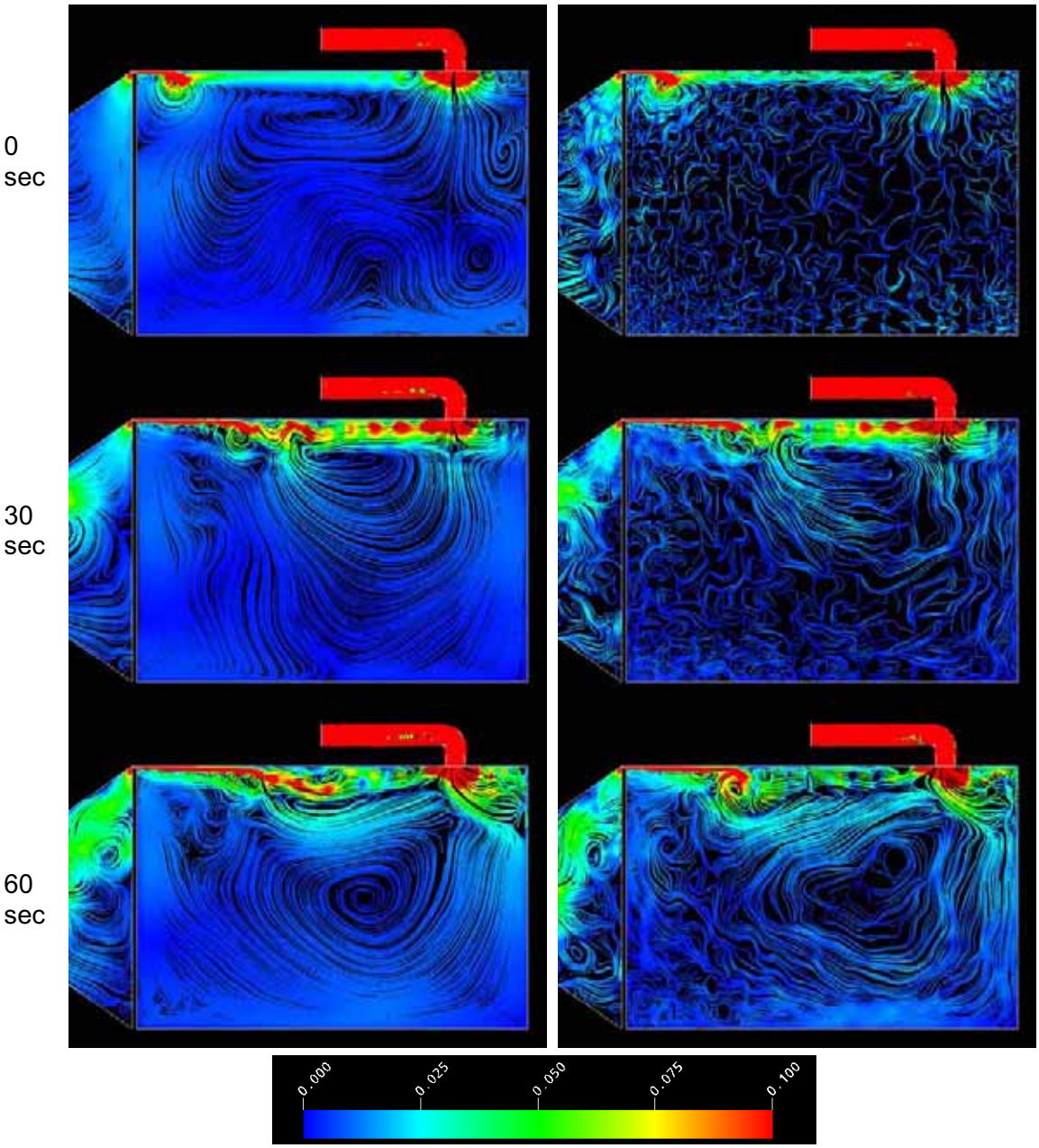

Figure 4 LES pre-calculations showing the flow development from two different initial conditions; on the left: a pure RANS solution; on the right: the same RANS solution superimposed with 0.01 m/s random fluctuations. Streamlines are shown on the mid-plane of the room coloured with the velocity magnitude.

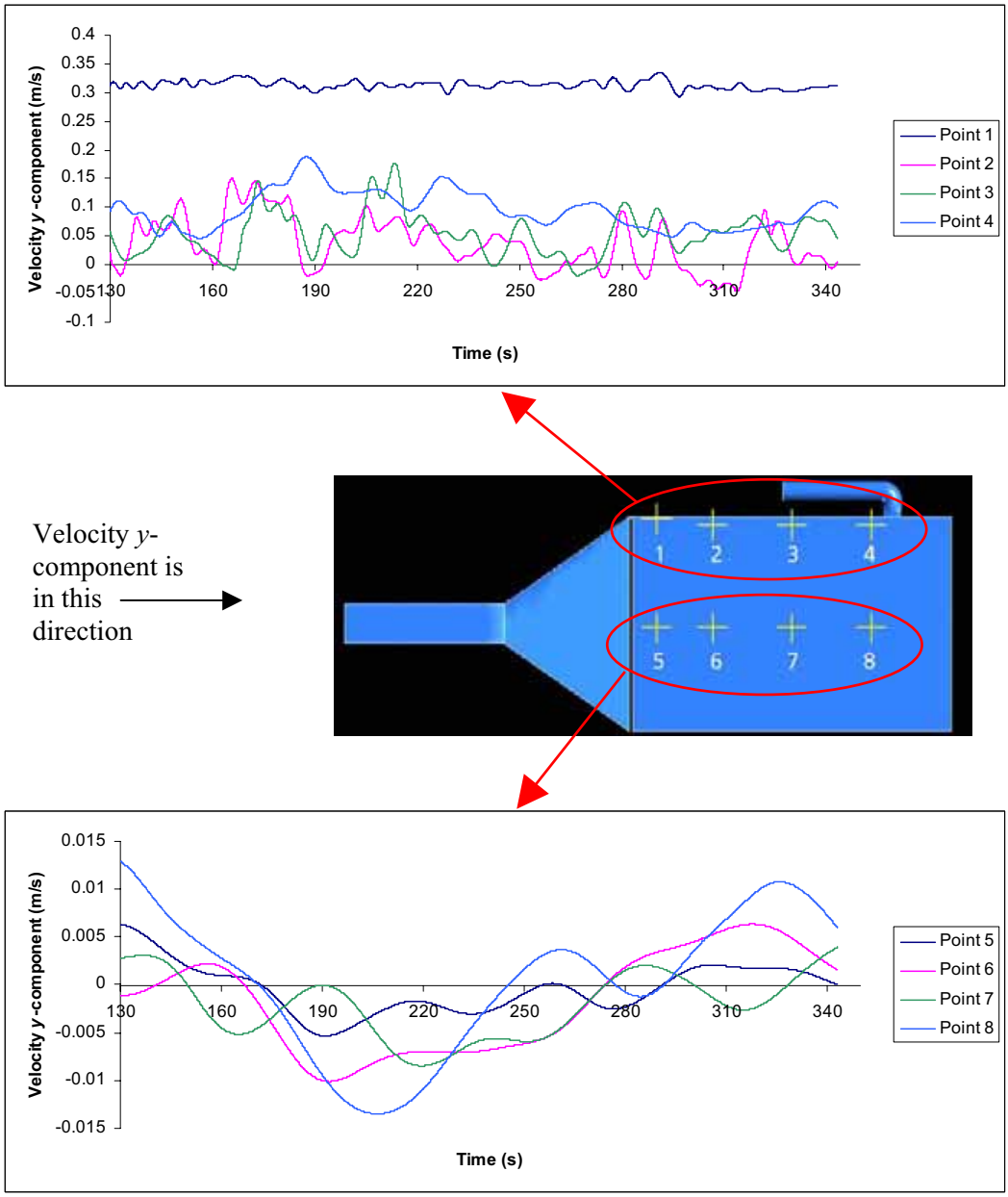

Figure 5 Variation of the y-component of velocity at 8 monitoring locations for the LES pre-calculation.

In order to visualise the eddy structures in the initial conditions, Figure 6 shows iso-contours of the velocity gradient invariant, I, given by:

$$I = S^2 - \Omega^2$$

where S and Ω are the strain-rate and vorticity invariants, respectively. Results for the LES are compared to those from the SST RANS model. Iso-contours for $I = 0.2$ are coloured according to the ratio of turbulent to laminar viscosity.

The LES clearly shows considerably more fine-scaled flow structures than the RANS. Spanwise, roll-up vortices are present in the shear layer near the inlet to the room which evolve gradually into larger, less coherent eddy structures moving towards the exhaust duct. In the LES, the maximum subgrid-scale viscosity in the room is approximately 4 times the laminar viscosity whilst the viscosity ratio in the RANS simulation is considerably higher (up to $\nu_t/\nu \approx 60$).

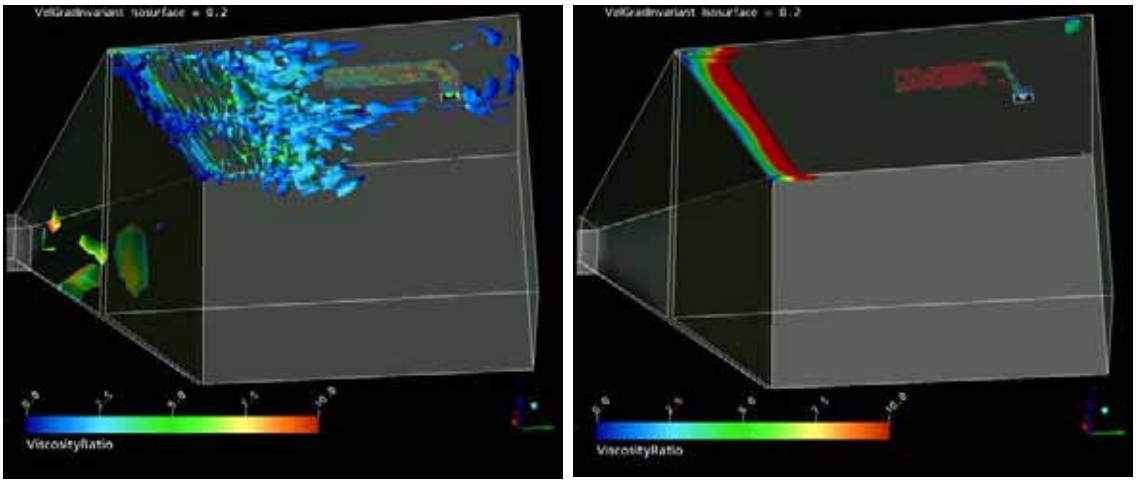

Figure 6 Iso-contours of the velocity gradient invariant, $I = 0.2$, for the LES (left) and RANS model (right). Contours are coloured with the ratio of turbulent to laminar viscosity.

3.4 RESULTS

Having established fully-developed flow conditions using the pre-calculation method, the contaminant gas concentration in the room was set to a value of 1.0 everywhere at a time $t = 0$ and the LES calculation continued for a further 1000 seconds of simulated time (from now on this calculation is denoted: LES1). The gas concentration was observed to gradually decrease in the room as clean air entered and the gas/air mixture was extracted. A similar calculation was performed using the SST RANS model[3]. Two further LES calculations were made. The first of these started from the velocity field of run LES1 at time $t = 500$ seconds and reset the contaminant gas field to a value of 1.0. The calculation was then continued for a further 500 seconds (this run is denoted: LES2). The third LES calculation (LES3) used a slightly different damping function in the turbulence model to treat the near-wall region of the flow, but used identical initial conditions to those used in run LES1. Again, this was run for 500 seconds. Details of the LES models used in calculations LES1, LES2 and LES3 can be found in the Appendix.

A comparison of the streamlines and gas concentration predicted by the LES and RANS models after approximately 1000 seconds is shown in Figure 7. The time-history of gas concentration at a single point in the room, just below the exhaust duct, for all four calculations is shown in Figure 8.

[3] *A separate pre-calculation was performed using the SST model to obtain fully-developed initial flow conditions.*

Figure 7 shows that the flow predicted by the RANS model features a large, coherent, recirculation in the upper half of the room, stretching most of the way from the inlet to the exhaust duct. In contrast, the LES result shows a complex and disordered collection of smaller eddy structures. Both models predict large eddy structures in the lower half of the room, the RANS slightly less so than the LES. The actual flow velocities in this region of the flow were very low, typically below 0.01 m/s (0.02 miles/hr). The colour of the streamlines in Figure 7 indicates that the gas concentration predicted by the RANS and LES models are similar, despite the differences in the flow field.

Figure 8 shows that the overall trend in predicted gas concentrations near the exhaust was similar in the LES and RANS model results. The three LES results provide some indication of the likely statistical scatter in gas concentrations about the mean level. From $t = 0$ to $t = 200$ seconds, the mean of the three LES results is slightly higher than that of the RANS. However, overall, there is good agreement between the mean LES and RANS results.

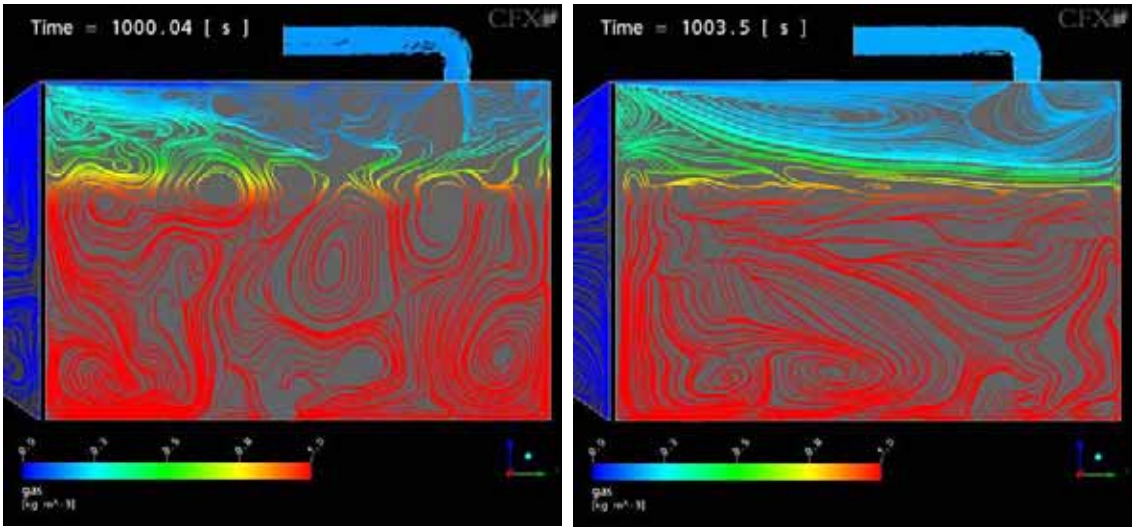

Figure 7 Streamlines on the mid-plane coloured with the contaminant gas fraction after approximately 1000 seconds from the gas release as predicted by LES (left) and SST RANS model (right). Both results shown are snapshots taken at a single instant in time.

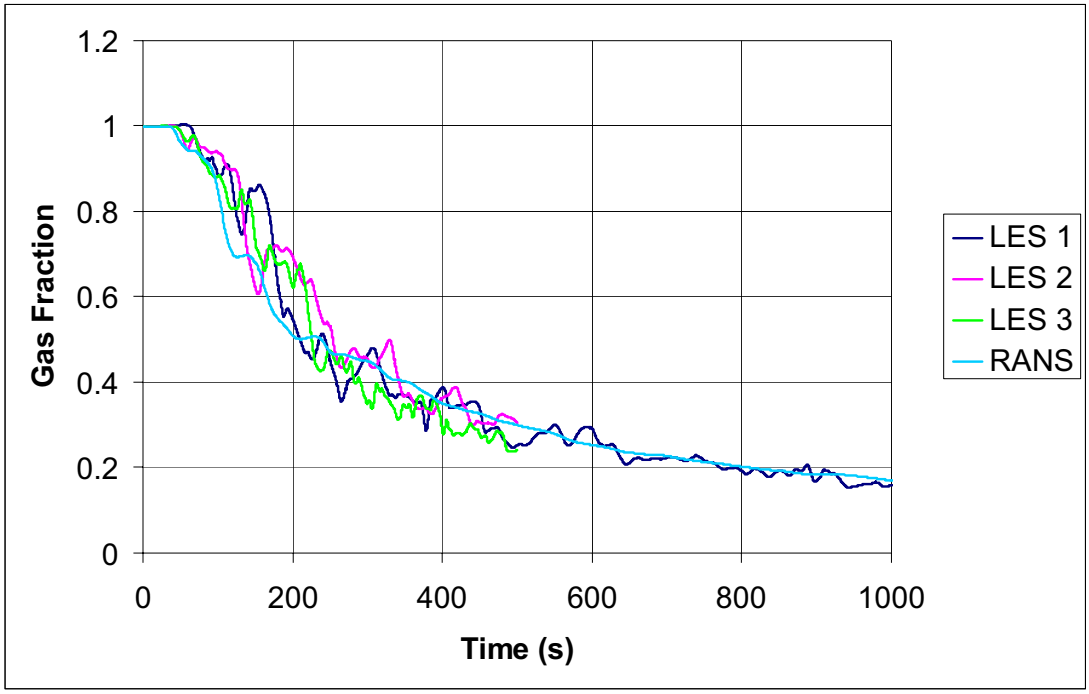

Figure 8 Variation of the contaminant gas fraction near the exhaust duct over time for three separate LES calculations (LES1, LES2 and LES3) and an SST-model RANS calculation. Calculations LES2 and LES3 were only run for 500 seconds.

3.5 COMPUTING TIMES

The total computing time taken for calculating 1000 seconds of simulated time using LES was around two and a half weeks. This excludes the time taken for the pre-calculation, to obtain the initial conditions. For part of this time the simulation was run on a single processor and at other times it was run in parallel using 2 processors on a 3.6GHz Xeon desktop PC.

Comparisons of computing times for the LES calculations using 1 and 2 processors, and three different RANS model calculations are presented in Table 1. The LES was approximately 5 times slower per second simulated time than the SST RANS model for the same number of processors. This difference was mainly due to the time-step used in the LES being 10 times smaller than that used by the SST model[4]. All the present calculations (both RANS and LES) used the same computational mesh. Usually, LES requires a finer grid than RANS, in which case the difference in computing times between RANS and LES is more marked.

---

[4] *The difference is not simply a factor of 10 since the Smagorinsky LES model only solves five transport equations: three for velocity, a pressure-correction equation and an energy equation, whereas the SST model solves seven transport equations in total.*

Table 1 Comparison of computing times for LES and RANS models using 1 and 2 processors.

Model	*CPU Seconds per Simulated Second*	*Relative Times*
RANS – SST (2 processors)	261	1.0
RANS – SST (1 processor)	369	1.4
RANS – DSM (1 processor)*	496	1.9
LES (2 processors)	1299	5.0
LES (1 processor)	1922	7.4

* The Differential Stress Model (DSM) calculations were run using the same flow scenario and computational grid at a slightly lower ventilation rate (0.5 ach). See Gobeau *et al*. [2] for details.

3.6 EVALUATION OF SPATIAL AND TEMPORAL RESOLUTION

In Section 2, four parameters were identified for use in evaluating the spatial and temporal resolution of large-eddy simulations. Plots of each of these parameters are presented below.

The ratio of turbulence length scales to grid cell dimensions, shown in Figure 9, gives a slightly misleading impression of the grid resolution. It is calculated from:

$$\frac{(Vol)^{1/3}}{k^{3/2}/\varepsilon}$$

where *Vol* is the cell volume and k and ε are values of the turbulence kinetic energy and dissipation rate taken from the SST RANS solution. Ideally, according to the analysis of Baggett *et al*. [12], the ratio should be less than 0.1 for well-resolved LES. Away from the turbulent wall jet along the ceiling of the room, the SST model predicts the flow to be mostly laminar. The value of $k^{3/2}/\varepsilon$ therefore falls to zero and the above ratio tends to infinity. At first glance, Figure 9 then shows that the grid is overly coarse as the ratio is significantly greater than 0.1 across most of the domain. In fact, most of the regions of the flow where the ratio is larger than 0.1 are laminar – and hence may be adequately resolved. This confusion arises from the use of a RANS turbulence length scale in a flow that is transitional. Near the ceiling in the room, where the flow is fully turbulent, the above ratio varies between 0.1 and 0.5. This indicates that the grid is probably too coarse in this region.

Figure 10 shows contours of y^+, the dimensionless wall-normal distance, for both the SST and LES models on the surfaces of the room. For both models, the predicted y^+ is larger than 10 along part of the ceiling and the upper part of the side walls. Over much of the rest of the domain, the y^+ is approximately 5 for the LES and around 2 with the SST model. For well-resolved boundary layers the y^+ should be less than one using LES. This indicates again that the

grid is rather coarse, for the LES at least. The SST simulation used a scalable wall function that should give reasonable predictions for the range of y^+ shown in the Figure. The difference between the predicted y^+ using the SST and LES models suggests that one should be careful using only RANS model results to assess the near-wall grid resolution.

Plots of the Courant number using the LES and RANS models are shown in Figure 11. The LES calculation used a time step of Δt = 0.05 seconds whilst the RANS used Δt = 0.5 seconds. However, for the purposes of creating Figure 11, the Courant number has been calculated using Δt = 0.05 seconds for both LES and RANS. To minimize artificial numerical damping, the Courant number should be less than one everywhere. Over the vast majority of the domain this is the case, there is only a small region near the inlet where C exceeds one. The two results are in good agreement overall, suggesting that a prior RANS result could be used to judge whether the time-step is appropriate for LES.

Three alternative methods were presented in Section 2 for calculating the modelled subgrid-scale turbulence energy, k_s: the UL approach, Pope's method and Mason & Callen's method. It was shown that the Pope and Mason & Callen methods were similar whilst the UL method estimated k_s to be nearly two-orders of magnitude smaller. Figure 12 shows contours of the ratio of the modelled to the total turbulent kinetic energy using the UL and Pope approaches (the Mason & Callen results, not shown, are similar to the Pope results). The red contours indicate that 50% of the turbulence energy is modelled. Using the UL method, the proportion of turbulence energy modelled is practically zero across most of the room. In contrast, the Pope method predicts an average of about 25% modelled in the upper half of the room and a few patches where the ratio exceeds 50%. WS Atkins [14] and Pope [11] suggested that less than 20% should be modelled for well-resolved LES. Depending on which method one chooses to calculate k_s, one can agree or disagree with this criterion. This matter should be clarified in future work.

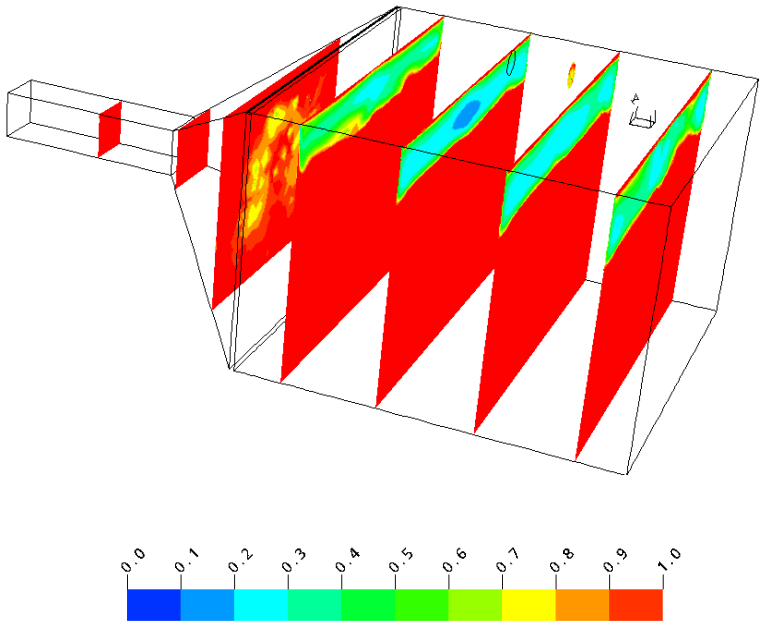

Figure 9 Contours of the ratio of turbulence length scales to grid cell dimensions for the SST model.

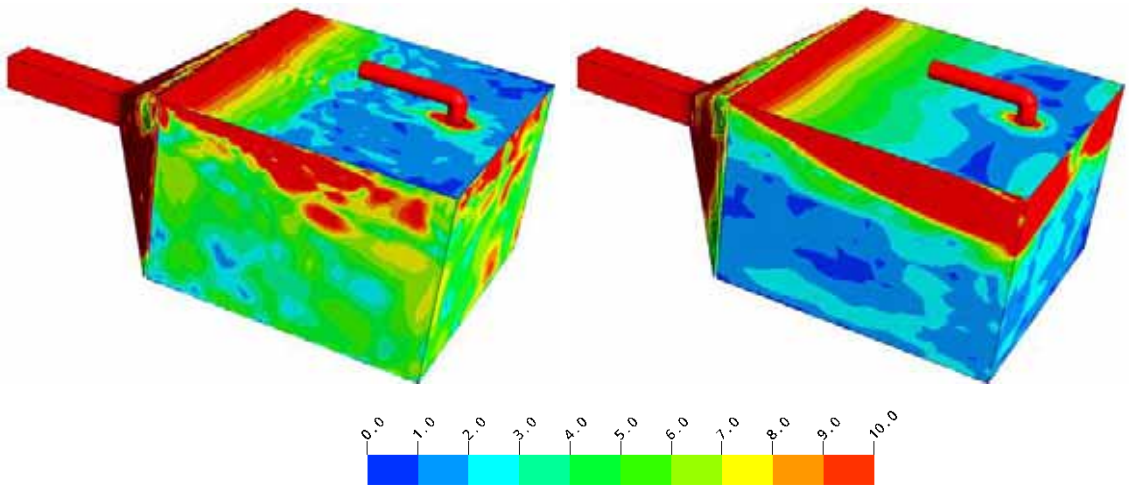

Figure 10 Dimensionless wall-normal distances (y^+) for the LES (left) and the SST model (right). Both results shown are for a single instant in time.

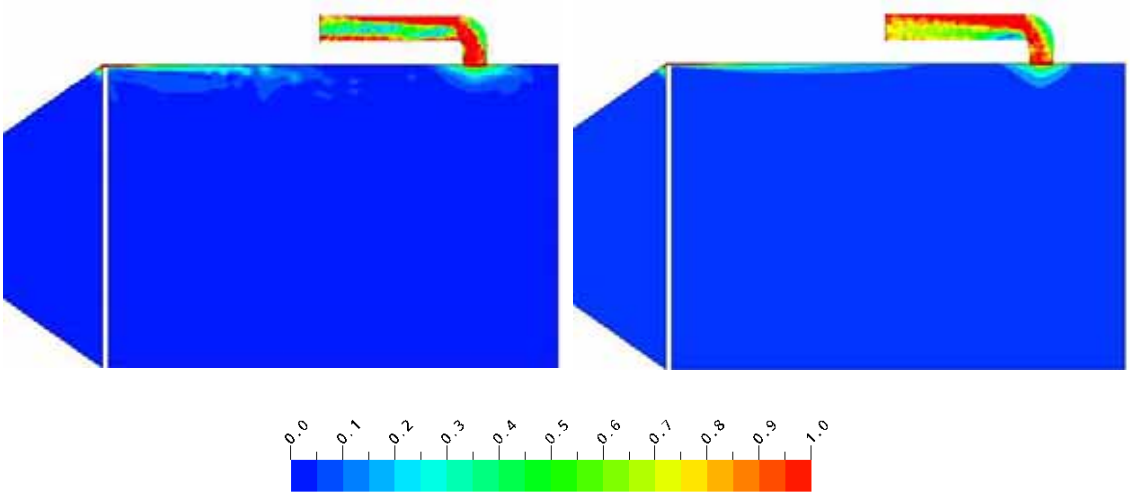

Figure 11 Contours of the predicted Courant number, *C*, on the mid-plane using LES (left) and the SST model (right). In both cases, the time-step used to calculate *C* is Δt = 0.05 seconds.

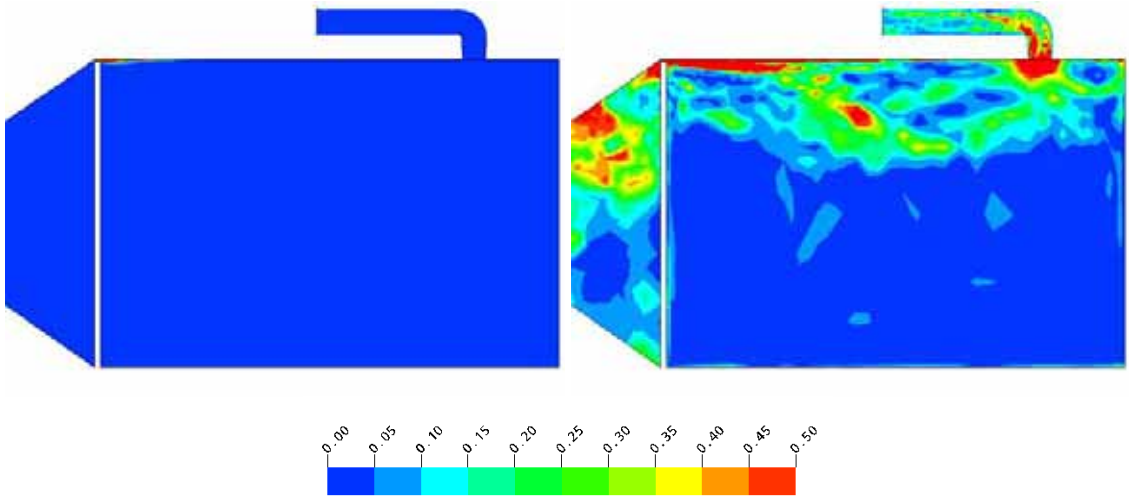

Figure 12 Contours of the ratio of modelled to total turbulence kinetic energy using the UL calculation method (left) and Pope method (right). Both results are for the LES calculation.

4 CONCLUSIONS

A preliminary study has been made of gas dispersion in a room using Large-Eddy Simulation (LES). This has shown that LES can provide information on the statistical spread in gas concentration and data on peak levels. Such data cannot easily be extracted from Reynolds-averaged Navier-Stokes (RANS) models. In some applications, such as assessing exposure to highly toxic vapours, it is essential to have accurate data on peak and instantaneous concentration levels. LES is well-suited to the simulation of these scenarios.

A number of different criteria have been investigated to determine the spatial and temporal resolution of the LES results. There is still some uncertainty in using one of these parameters, namely the ratio of the modelled kinetic energy to the total kinetic energy. This parameter provides an indication of the spatial resolution, i.e. whether the LES is resolving all the large eddies or just the *very* large eddies. The uncertainty over the calculation method should be clarified in future work. The measure would provide an indicator of the quality of LES results which would be particularly useful in assessing third-party LES. Overall, the conclusions from the study were that the temporal resolution was adequate but the grid used was probably too coarse. The computing times for these simulations, given in Section 2, indicate that a repetition of the simulations using a refined grid would require a substantial computing effort. Even at present, to simulate 1000 seconds required more than two weeks computing time. Parallel computing could have reduced this, however.

It seems clear from this study that LES will not supplant RANS in the immediate future for modelling gas dispersion. Many of the gas dispersion cases faced by HSE are ad-hoc and ill-defined. The modelling process therefore needs to examine the sensitivity of CFD predictions to changes in the unknown operating conditions (temperatures, flow rates, dispersion properties etc.) and the requirements of the case under consideration. Typically this may involve a dozen or more separate simulations. Performing this number of simulations using LES would require very long computing times. However, LES is well suited to providing detailed information on particular, well-defined test cases. It is already being used to help support safety cases and its use is likely to become more widespread as computers become more powerful and sufficiently cheap to be run in parallel. It is recommended that expertise in LES be developed and maintained. In cases where detailed exposure assessments need to be made, LES should be considered as an alternative or complement to existing RANS models.

5 APPENDIX: LES MODEL DETAILS

The Smagorinsky LES model [19] has been used in the present work. Subgrid-scale stresses, τ_{ij}, are expressed in Cartesian tensors as follows:

$$\tau_{ij} - \frac{1}{3}\delta_{ij}\tau_{kk} = -2\nu_t S_{ij}$$

where δ_{ij} is the Kronecker delta, S_{ij} is the strain rate tensor and ν_t is the subgrid-scale viscosity, given by:

$$\nu_t = \min\left(l_{mix}, f_\mu c_s \Delta\right)^2 |S|$$

The Smagorinsky coefficient, c_s, is a constant (taken as 0.1 in the present work), S is the strain-rate invariant, Δ is the filter-width and f_μ is a near-wall damping function. In calculations LES1 and LES2, f_μ has been assumed to be equal to 1.0. In calculation LES3, the following van Driest function was used:

$$f_\mu = 1 - \exp\left(\frac{y^+}{A}\right)$$

where y^+ is the dimensionless wall distance and A is a constant, taken as 25.

In all the calculations, the mixing length, l_{mix}, was calculated from:

$$l_{mix} = \kappa y$$

where y is the wall distance and κ a constant, equal to 0.4.

Away from walls, the subgrid-scale viscosity asymptotes to:

$$\nu_t = \left(c_s \Delta\right)^2 |S|$$

6 REFERENCES

1. Gobeau, N. and C.J. Saunders. *Computational fluid dynamics validation of the prediction of pesticide dispersion in a natually-ventilated building*. in *Proc. 8th Int. Conference on Air Distribution in Rooms (Roomvent 2002) pp. 697-700.* 2002. Copenhagen, Denmark.

2. Gobeau, N., A. Kelsey, C.J. Saunders, and Y. Sinai. *Thermal effects on the dispersion of a gaseous contaminant in a natually-ventilated room*. in *Proc. 9th Int. Conference on Air Distribution in Rooms, Roomvent 2004*. 2004. Coimbra, Portugal.

3. Spalart, P.R., *Strategies for turbulence modeling and simulations.* Int. J. Heat Fluid Flow, 2000. **21**: p. 252-263.

4. Ledin, H.S., M.J. Ivings, J.T. Allen, and R.J. Bettis, *Evaluation of CFD modelling of smoke movement in complex enclosed spaces - production of small-scale experimental data and assessments of CFD*. 2004, Health & Safety Laboratory Report CM/04/07.

5. Ivings, M.J., M. Azhar, C. Carey, C.J. Lea, S. Ledin, Y. Sinai, C. Skinner, and P. Stephenson, *Outstanding Safety Questions Concerning the Use of Gas Turbines for Power Generation: Final Report on the CFD Modelling Programme of Work*. 2003, Health & Safety Laboratory Report CM/03/08.

6. Peng, S.-H., S. Holmberg, and L. Davidson, *On the assessment of ventilation performance with the aid of numerical simulations.* Building & Environment, 1997. **32**(6): p. 497-508.

7. Davidson, L., P.V. Nielsen, and C. Topp, *Low-Reynolds number effects in ventilated rooms: a numerical study.* Proc. 7th Int. Conference on Air Distribution in Rooms (Roomvent 2000), 2000: p. 307-312.

8. Emmerich, S.J. and K.B. McGrattan, *Application of a large eddy simulation model to study room airflow.* ASHRAE Transactions, SF-98-10-2, 1998. **104**.

9. Wang, H., R.N. Colvile, C.C. Pain, C.R.E. De Oliveira, and E. Aristodemou. *Airflows in the vicinity of an intersection*. in *9th Int. Conf. on Harmonisation with Atmospheric Dispersion Modelling for Regulatory Purposes*. 2004. Garmisch-Partenkirchen.

10. Davidson, L. and P.V. Nielsen. *Large eddy simulations of the flow in a three-dimensional ventilated room*. in *Proc. 5th Int. Conference on Air Distribution in Rooms (Roomvent '96)*. 1996. Yokohama, Japan.

11. Pope, S.B., *Turbulent Flows*. 2000: Cambridge University Press.

12. Baggett, J.S., J. Jiménez, and A.G. Kravchenko, *Resolution requirements in large-eddy simulations of shear flows*, in *Annual Research Briefs*. 1997, Stanford Centre for Turbulence Research.

13. Addad, Y., S. Benhamadouche, and D. Laurence, *The negatively buoyant wall-jet: LES results.* Int. J. Heat Fluid Flow, 2004. **25**: p. 795-808.

14. Cowan, J.R. and P. Gallagher, *Review of the applicability of the large eddy simulation technique to safety studies*, in *WSA Report AM5226/R1*. 1999, WS Atkins Science & Technology.

15. Mason, P.J. and N.S. Callen, *On the magnitude of the subgrid-scale eddy coefficient in large-eddy simulations of turbulent channel flow.* J. Fluid Mech., 1986. **162**: p. 439-462.

16. Kempf, A., R.P. Lindstedt, and J. Janicka, *Large-eddy simulation of a bluff-body stabilized nonpremixed flame.* Combustion and Flame, 2006. **144**: p. 170-189.

17. Morinishi, Y., T.S. Lund, O.V. Vasilyev, and P. Moin, *Fully conservative higher order finite difference schemes for incompressible flow.* J. Comput. Phys., 1998. **143**: p. 90-124.

18. Mittal, R. and P. Moin, *Suitability of upwind-biased finite difference schemes for LES of turbulent flow.* AIAA Journal, 1997. **35**(8): p. 1415-1417.

19. Smagorinsky, J., *General circulation experiments with the primitive equations.* Monthly Weather Review, 1963. **91**(3): p. 99-164.